



Electrochemically produced responsive hydrogel films: Influence of added salt on thickness and morphology

Johanna Bünsow, Diethelm Johannsmann*

Institute of Physical Chemistry, Clausthal University of Technology, Arnold-Sommerfeld-Strasse 4, 38678 Clausthal-Zellerfeld, Germany

ARTICLE INFO

Article history:
Received 10 June 2008
Accepted 8 July 2008

Keywords:
Smart hydrogel
N-isopropylacrylamide
Hofmeister series
Electrochemically induced polymerization
Added salt
Lower critical solution temperature
Surface morphology

ABSTRACT

We report on electrochemically prepared hydrogel layers of poly-*N*-isopropylacrylamide (pNIPAm) and on the influence that the supporting electrolyte has on their thickness and morphology. Ions that are destabilizing in the Hofmeister sense increase the thickness. The effect correlates well with the ion's tendency to lower the lower critical solution temperature (LCST) of pNIPAm films. AFM micrographs show small-scale globules. When the films were produced in the presence of a destabilizing salt (such as ammonium sulfate) one also observes larger features, resembling wrinkles. We attribute the globules to nucleated growth of surface-attached microgels, whereas the wrinkles presumably are produced by the collapse of hydrogen bubbles underneath a well-crosslinked film. Adding a chain transfer agent to the reactant solution reduces the lateral heterogeneities.

© 2008 Elsevier Inc. All rights reserved.

1. Introduction

Responsive hydrogels have received much interest as key elements in chemical sensors [1,2], bioanalytics [3], tissue engineering [4], and drug release [5,6]. Responsiveness here mostly implies a reversible volume-phase transition on changes of environmental parameters such as temperature or pH. The most prominent example of a responsive hydrogel is poly-*N*-isopropylacrylamide (pNIPAm), which has a lower critical solution temperature (LCST) of 32 °C [7]. Usually, the swelling/deswelling transition of pNIPAm gels in water is driven by temperature, but other parameters such as pH [8], cosolvents [9], and added salt [10] can also induce a collapse.

Hydrogels can be attached to solid supports by various techniques, including photo crosslinking of preformed polymer chains [11], initiation of a polymerization from self-assembled monolayers [12], atom transfer radical polymerization (ATRP) [12], and plasma polymerization [13]. Of particular relevance to this work are electrochemical methods. For example, Palacin and co-workers have grafted vinylic monomers to metal surfaces from anhydrous solutions [14,15]. This technique is based on an anionic polymerization and leads to a covalent link between the polymer and the substrate. Physisorbed hydrogels of various compositions can be prepared by an electrochemically induced precipitation [16]. Here, the polymer backbone contains acidic moieties. On application of a

positive potential to the electrode, the near-surface pH decreases, inducing protonation of the acidic moieties. The neutral polymer then readily precipitates onto the surface.

Electrochemically induced polymerization is a particularly flexible and simple way to produce hydrogel coatings [17–22]. Polymerization is triggered by the decomposition of an electro-active initiator at the cathode. The electron transfer produces a radical anion, which subsequently initiates a free radical polymerization. Since the film is produced in situ, the material adapts to the local roughness of the surface. The films usually adhere to the electrode very well. Delamination has never been observed on storage in water, even over months.

Generally speaking, addition of salts may both decrease and increase the LCST of pNIPAm. Depending on an ion's chemical nature, it may either destabilize or stabilize the dissolved chains. When arranging different salts in a series according to the shift in the LCST, one finds the Hofmeister series reproduced. The latter was originally devised to quantify the extent by which electrolytes induce coagulation of hen egg white albumin [23]. At concentrations below 0.2 mol/L, the anions are arranged in the order $\text{CO}_3^{2-} > \text{SO}_4^{2-} > \text{S}_2\text{O}_3^{2-} > \text{H}_2\text{PO}_4^- > \text{F}^- > \text{Cl}^- > \text{NO}_3^- \approx \text{Br}^- > \text{ClO}_4^- > \text{I}^- > \text{SCN}^-$, where ions on the left decrease the LCST, whereas ions on the right increase it [24]. The mechanisms underlying the Hofmeister series are under debate. There is a delicate balance between hydrogen bonding, entropy, and hydrophobic interactions. Traditionally, the Hofmeister series was attributed to the way in which an ion modifies the local arrangement of water. Different ions were believed to be either “structure making” or “structure breaking” [25]. Recent experiments raised doubt on that view [26,27].

* Corresponding author. Fax: +49 5323 72 4835.

E-mail address: johannsmann@pc.tu-clausthal.de (D. Johannsmann).

For instance, it was found that the salt's partial compressibility did not correlate well with the ion's effect on protein coagulation. This would have been expected if the local water structure was the determining factor. Dispersion forces have been proposed as having much influence, as well [27,28]. There are many different phenomena that are affected by an ion's position on the Hofmeister scale, including protein aggregation, catalytic activity of enzymes, surface tension, critical micelle concentration, and others [23]. Here, we report on a further example, which are the thickness and the morphology of hydrogel films produced by electrochemically triggered free radical polymerization.

An influence of the solvent employed in preparation on the properties of hydrogels has been studied before. For example, Suzuki et al. report that pNIPAm films were rather rough when produced in water at temperatures above the LCST, which they explain with fast precipitation [29]. Sayil and Okay measured the swelling ratio of pNIPAm hydrogels [30] and found the swelling ratio to be correlated with the temperature at the time of preparation. They argue that the number of elastically effective crosslinks is low in situations where a growing chain readily collapses onto itself. A related phenomenon was observed by Lee and Yen, who studied the swelling ratio obtained after polymerizing in different media [31]. Employing water/acetone or water/ethanol mixtures, they found the swelling ratio to increase with decreasing water content. They suggest that pores are created when forming the gel in the presence of an organic cosolvent due to preferential solvation.

Recently, Ishida and Biggs investigated the influence of sodium sulfate on the morphology of grafted pNIPAm chains by AFM and QCM with dissipation monitoring (QCM-D) [32]. At a certain concentration of sodium sulfate, the morphology of the films changed from a flat to a mushroom-like structure when immersed into the salt solution. Jhon et al. measured the volume phase transition of pNIPAm brushes by QCM-D [33]. They found a decrease of the LCST with increasing salt concentration. In contrast to free pNIPAm chains in solution, the LCST of grafted pNIPAm chains decreased nonlinearly with increasing salt concentration.

We are not aware of work on the effect that addition of salt during the preparation stage has on the properties of surface-attached pNIPAm gels. Added salt is an important parameter because electrochemical preparation requires a supporting electrolyte in order to conduct the current. We report a comparison of the effects that two salts (ammonium sulfate and ammonium perchlorate) of varied concentrations have on the film thickness, the surface morphology, and on the LCST of the films. Further, we have employed a chain transfer agent. The lateral heterogeneity can be much reduced in this way, which should be of practical relevance.

2. Materials and methods

2.1. Materials

Ammonium sulfate (Fluka), ammonium perchlorate (Alfa Aesar), ammonium nitrate (Acros Organics), ammonium persulfate (Sigma Aldrich), and *N,N'*-methylenebisacrylamide (BIS, Merck) were used as received. *N*-isopropylacrylamide (NIPAm, Acros Organics) was purified by triple recrystallization from hexane and dried under vacuum before use.

2.2. Electrochemically initiated polymerization

The pNIPAm films were produced on the front electrode of an electrochemical quartz crystal microbalance (EQCM). The EQCM allows for in situ monitoring of the frequency shift, Δf , and the shift of half-bandwidth at half-maximum, $\Delta \Gamma$ ("bandwidth," for short),

during the polymerization by means of impedance analysis. Resonance curves were fitted to the admittance spectra acquired with a network analyzer (HP4396A, Hewlett Packard). The frequency shifts were converted to a film thickness with the Sauerbrey equation

$$\Delta f = -\frac{2nf_f^2}{Z_q}m_S = -\frac{2nf_f^2}{Z_q}\rho_f d_S, \quad (1)$$

where f_f is the frequency of the fundamental, n is the overtone order, $Z_q = 8.8 \times 10^6 \text{ kg}/(\text{m}^2 \text{ s})$ is the acoustic impedance of AT-cut quartz, m_S is the mass per unit area of the film, $\rho_f = 1 \text{ g}/\text{cm}^3$ is the density of the film [34], and d_S is the film thickness in the Sauerbrey sense (called "Sauerbrey thickness"). The reference states were the frequencies of the bare crystal measured in air or in the reactant solution. When a film is immersed in a liquid, the Sauerbrey equation does not necessarily yield the geometric thickness because of viscoelastic effects. Also, the film may contain trapped solvent. Both m_S and d_S therefore are effective parameters. The subscript "S" (for Sauerbrey) emphasizes this caveat.

The polymerization was performed under potentiostatic control (PGU 10V-1A IMP, Jaissle, Germany or Iviumstat, EKTechnologies, Germany) in a three-electrode setup with a platinum counter electrode, a saturated calomel reference electrode (SCE, Sensortechnik Meinsberg, Germany), and the front electrode of a gold-coated 5 MHz AT-cut quartz crystal (Maxtek Inc., Santa Fe Springs, CA) as the working electrode. All potentials are relative to SCE.

The crystals were first cleaned in a UV/ozone cleaner (Bioforce Nanosciences, USA) for 15 min. Subsequently, they were electrochemically cleaned in 1 M sulfuric acid by cycling the potential from 0 to -1 V at a rate of $10 \text{ mV}/\text{s}$ for 2 to 3 h. The reactant solution contained NIPAm (0.3 mol/L, the monomer), ammonium persulfate (12.5 mmol/L, initiator), and BIS (3 mmol/L, crosslinker). These chemicals were dissolved in ultrapure water (arium 611VF, Sartorius, Germany). Supporting electrolyte (ammonium sulfate, ammonium nitrate, or ammonium perchlorate) was added at concentrations between 0.25 and 0.6 mol/L. The solution was filtered with a $0.2 \mu\text{m}$ PVDF filter (Titan, USA) before injection into the cell. Prior to polymerization, the solution was bubbled with nitrogen for 10 min. Before and after each measurement a cyclovoltammogram (-1 to 0 V , $100 \text{ mV}/\text{s}$) was acquired. Polymerization was triggered by application of -0.8 V vs SCE for 15 min. After preparation, the films were extensively rinsed and stored in ultrapure water at 8°C .

2.3. Determination of the LCST

A quartz crystal coated with a pNIPAm film was mounted in a home-built liquid cell and placed onto a heating stage. The sample was heated from room temperature to 50°C at a rate of $0.08^\circ \text{C}/\text{min}$ in water and in aqueous solutions of ammonium sulfate, ammonium nitrate, and ammonium perchlorate. The LCST was inferred from the temperature dependence of Δf and $\Delta \Gamma$ [17].

2.4. AFM measurements

Because the quartz crystals were too large for the sample compartment of the AFM available to us, separate samples were prepared on small substrates for AFM imaging. The substrates were glass slides, coated with gold and a thin layer of chromium as an adhesion promoter between the glass and the gold. Prior to polymerization, the substrates were cleaned in a UV/ozone cleaner for 15 min. After drying, the films were imaged with an AFM (extended multimode, NanoScope IIIa controller, Veeco/Digital Instruments) operating in tapping mode at room temperature in air.

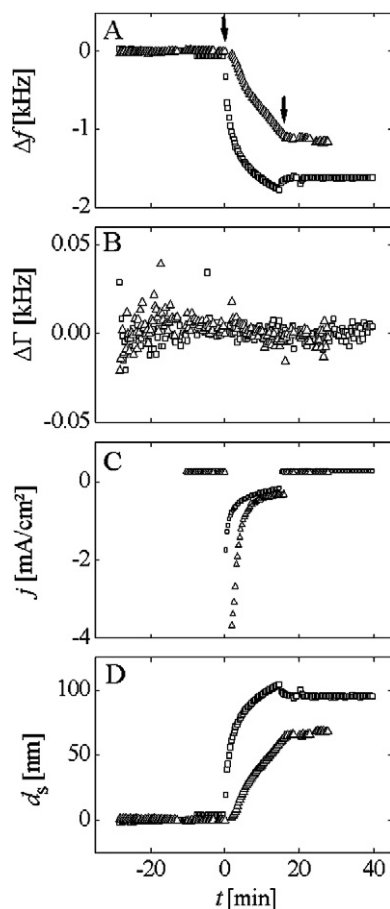


Fig. 1. Frequency shift Δf (A), bandwidth shift $\Delta\Gamma$ (B), both measured on the 15 MHz overtone, current density j (C), and Sauerbrey thickness d_s (D) obtained in reactant solutions containing 0.6 mol/L of $(\text{NH}_4)_2\text{SO}_4$ (squares) or NH_4ClO_4 (triangles). The polymerization was triggered by applying a potential of -0.8 V for 15 min (arrows in panel A). Added salt affects the growth kinetics and the final film thickness.

3. Results and discussion

Fig. 1 shows a typical set of frequency shifts (Δf , panel A), shifts in dissipation ($\Delta\Gamma$, panel B), and current density (j , panel C) during polymerization of NIPAM in aqueous solutions of 0.6 M ammonium sulfate and 0.6 M ammonium perchlorate. Panel D in Fig. 1 shows the film thicknesses, d_s , obtained from the frequency shifts by application of the Sauerbrey equation (Eq. (1)). The formation of pNIPAM is fast, initially, but slows down after some minutes as indicated by a kink in the frequency shift (panel A). This kink shows that a film forms at the surface and slows down the further polymerization. Presumably, the film acts as a barrier to the diffusion of the initiator toward the electrode. This hypothesis is supported by the decrease of the current density during EIP (see panel C). The slowing down of the growth rate with time is less pronounced in perchlorate solution than in sulfate, indicating that the former films more easily allow for diffusion of reactants to the electrode surface. The barrier properties of any given film are governed by the thickness and by the density. Presumably, films formed from perchlorate solution are less dense than films formed from sulfate solutions. The final wet film thicknesses were 95 and 69 nm in sulfate and in perchlorate solution, respectively. After the voltage was turned off, a short deswelling period was observed in the sulfate solution as indicated by a small increase in frequency. Evidently, a swelling equilibrium had not been reached during polymerization. The deswelling may either be attributed to the release of trapped water from the network or to the collapse

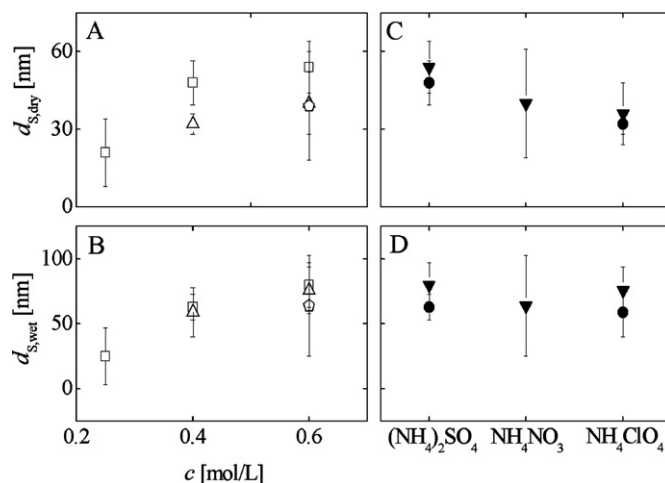


Fig. 2. Dry and wet thickness of pNIPAM films produced in solutions of $(\text{NH}_4)_2\text{SO}_4$ (open squares), NH_4NO_3 (open pentagons), and NH_4ClO_4 (open triangles) plotted versus the electrolyte concentration (A, B). All data are mean values determined from at least three experiments. Error bars are standard deviations. Both the wet and the dry film thicknesses increase with increasing concentration of the supporting electrolyte. When plotting the dry and the wet film thickness versus the type of salt (C, D), the dry thickness decreases in the order sulfate > nitrate > perchlorate. Full circles and full inverted triangles correspond to concentrations of 0.4 and 0.6 mol/L, respectively.

of small hydrogen bubbles formed underneath the film. The bandwidth shifts ($\Delta\Gamma$, panel B) are within the noise, which implies that the elastic stiffness of the films much exceeds the stiffness of the bulk. Different overtones yield the same Sauerbrey mass (data not shown), which also supports this conclusion. A hard film would typically be a collapsed film ($T > \text{LCST}$). The current density (j , panel C) peaks, initially, and then drops. Comparing the current density between the two cases, we find it to be smaller for polymerization in sulfate. In sulfate, a dense film forms quickly after the voltage is turned on. This film blocks the access to the electrode for monomer and/or initiator in a later stage more efficiently than the perchlorate film. We conclude that film formation is faster in sulfate solution because sulfate is the more destabilizing ion.

Fig. 2 shows the dry (A and C) and the wet (B and D) Sauerbrey thicknesses as a function of concentration (A and B) and the type of electrolyte (C and D). The data shown in Fig. 2 are averages over at least three experiments. The thickness positively correlates with concentration because added salt increases the tendency toward precipitation. The chemical nature is an influence, as well. Thicker films were produced in the presence of sulfate, which has a higher salting-out capability than perchlorate [24]. To check whether the film thickness follows the Hofmeister series, an additional experiment was carried out in the presence of 0.6 mol/L nitrate. The dry film thickness decreased in the order sulfate > nitrate > perchlorate, which is the expected sequence according to Hofmeister [24].

Fig. 3 displays the LCSTs as a function of the concentration (A) and the type of salt (B). For a low LCST ($< 25^\circ\text{C}$) the instrument can only determine an upper bound (arrows). The LCST decreases in the order $\text{H}_2\text{O} > \text{perchlorate} > \text{nitrate} > \text{sulfate}$. Only at 0.4 mol/L, perchlorate slightly increased the LCST. The ordering is similar to that reported by Zhang and co-workers in their studies on bulk pNIPAM [24]. The LCST order is in the same way as the film thickness. As the LCST is a measure of an electrolyte's capability to precipitate pNIPAM, we conclude that precipitation is the parameter that dominates the film thickness. In the following we focus on films prepared in the presence of sulfate and perchlorate which are the electrolytes with the highest and the lowest salting-out capability, respectively.

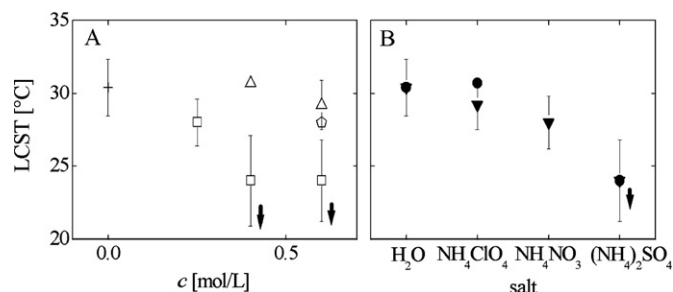


Fig. 3. (A) LCST of pNIPAm films in water (crosses) and in solutions of NH_4ClO_4 (triangles), NH_4NO_3 (pentagons), or $(\text{NH}_4)_2\text{SO}_4$ (squares) at various concentrations. (B) LCST of pNIPAm films versus the type of electrolyte. The concentrations are 0.4 (circles) or 0.6 mol/L (inverted triangles). The LCST decreases with concentration. Further, it decreases with increasing salting-out capability in the Hofmeister sense.

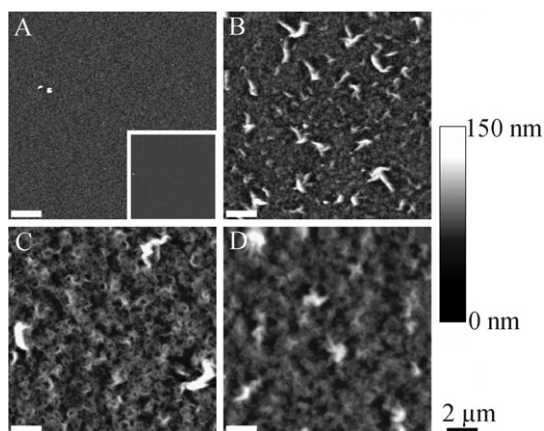


Fig. 4. AFM images from pNIPAm films produced in aqueous solutions of 0.4 and 0.6 mol/L NH_4ClO_4 (A, B) and of 0.25 and 0.6 mol/L $(\text{NH}_4)_2\text{SO}_4$ (C, D). The images were acquired on dry films in air using the tapping mode. The inset in panel A represents a bare gold surface which appears almost flat as compared to the pNIPAm films.

AFM micrographs taken on pNIPAm films prepared in different salt solutions are shown in Fig. 4. All images show some small-scale globules. These are *not* features originating from the underlying substrate. The inset in panel A shows a bare gold surface imaged under the same conditions. The bare gold appears almost flat as compared to the pNIPAm film, demonstrating that the globular features are indeed characteristic for the hydrogel. When polymerization was performed in 0.4 M ammonium perchlorate (image A), only the small globules are found. Somewhat larger, elongated protrusions are seen on samples polymerized at a higher concentration (0.6 M, image B), which we term “wrinkles.” The images of samples prepared in sulfate solutions (C and D) are dominated by wrinkles. Some of the samples also

exhibit depressions, resembling the remnants of pores or collapsed voids.

Figs. 5A and 5B are cartoon depictions which summarize the proposed mechanisms of structure formation. As long as the salting-out capability of the solvent is low, the AFM images only show small-scale globules (Fig. 5A). Presumably, these globules are formed in essentially the same way as in the bulk: Once a film has formed at some location, the likelihood that newly formed polymer chains stay in place (rather than diffusing away into the bulk) increases relative to the bare surface. A hydrogel film will trap the newly formed chains. Attachment of these chains to the existing matrix will readily occur. In addition, polymerization of NIPAm is an exothermic process, which accelerates precipitation. This would eventually amount to a positive feedback mechanism, leading to self-accelerating film growth, instabilities, and structure formation.

Wrinkles are found when the salting-out capability of the electrolyte is high (Fig. 5B). Once a dense hydrogel layer covers the surface, the access of the initiator to the surface is blocked. Hydrogen formation gains in relative importance and bubbles form underneath the hydrogel sheath. Hydrogen formation is evidenced by cyclic voltammetry in the reactant solution (data not shown). These cyclovoltammograms show an increase of the hydrogen peak in solvents with a high salting-out capability. Once the hydrogen bubbles reach a critical size, they produce blisters or even induce delamination. We interpret the wrinkles as collapsed blisters.

Interestingly, there is a way to drastically reduce the heterogeneity, which we report on as a side remark. In conventional polymerization reactions, the creation of very long chains and the formation of (accidental) crosslinks can be prevented by the addition of a chain transfer agent. Transfer agents employed in crosslinking copolymerization reduce the tendency toward microgel formation for this reason [35]. This mechanism works the same way for electrochemically triggered polymerization at a surface. Adding sodium formate to the reaction mixture generates films that are not only thicker than corresponding films created without sodium formate, but also more homogeneous. Fig. 6 displays two AFM images, which show the comparison. The basic recipe (Fig. 6A) was given by a reactant solution containing 0.3 M NIPAm, 0.25 M $(\text{NH}_4)_2\text{SO}_4$, 12.5 mM ammonium persulfate, 3 mM BIS, and 7.5 vol% of a 25% ammonia solution. The sample shown in Fig. 6B was created with essentially this recipe where 7.5 mM HCOONa was added. Because sodium formate is more active under basic conditions, we shifted the pH of the reaction to around 8.5 for both experiments (Figs. 6A and 6B) [36]. The film produced in the presence of a chain transfer agent is much smoother than the former. This finding supports the notion that the globules seen in Figs. 4A and 6A are indeed surface-attached microgel particles. Rapid chain transfer leads to the creation of a much larger number of short chains, which are distributed at the surface more evenly than long (and potentially crosslinked) chains. Evidently, crosslinking eventu-

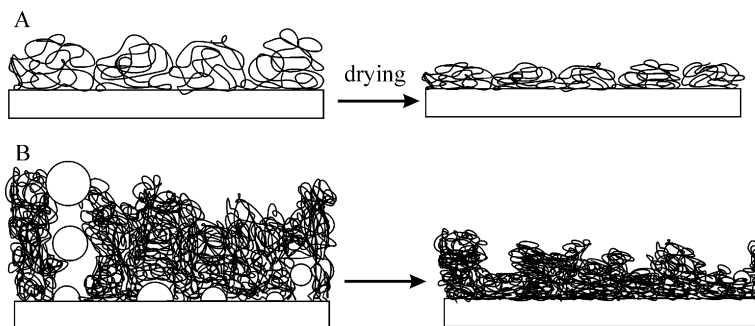


Fig. 5. Proposed mechanism of structure formation. (A) In electrolytes with a low precipitation capability, a loose network forms and homogeneous films consisting of small microgel domains are obtained. (B) When the film grows in a more collapsed state, hydrogen bubbles form underneath the film. The bubbles produce wrinkles on drying. If the film is strongly collapsed, hydrogen bubbles can reach the critical size for delamination, resulting in the formation of pores.

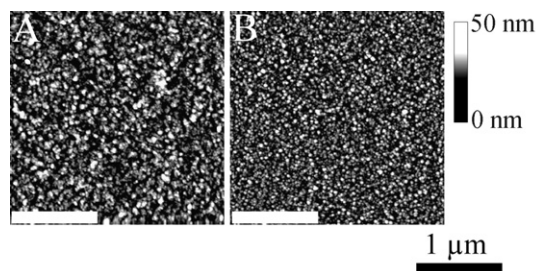


Fig. 6. Comparison of surface morphology obtained without (A) and with (B) addition of the chain transfer agent HCOONa (7.5 mM, pH \sim 8.5). The rms roughness was 4.98 and 4.22 nm with and without HCOONa, respectively.

ally happens due to the presence of the tetrafunctional monomer BIS, but at this time the film has spread out on the surface rather evenly.

4. Conclusions

The thickness and surface morphology of pNIPAm films produced by electrochemically induced polymerization depend on the nature and the concentration of the supporting electrolyte. The film thickness increased with increasing salt concentration and with increasing salting-out capability of the electrolyte. The salting-out capability of a certain salt onto the film was quantified via the shift of the LCST. The shift of the LCST decreased in the order sulfate > nitrate > perchlorate. The surface morphology showed small-scale globules in the case of low salting-out capability. When the tendency for precipitation became stronger, the films displayed wrinkles and holes. We attribute the globular structures to surface-attached microgels and the larger structures to the remnants of blisters formed from hydrogen gas. Globule formation can be much reduced by addition of a chain transfer agent to the reactant solution.

Acknowledgments

We thank B. Kusssmaul and R. Elze for preliminary studies, W. Oppermann for stimulating discussions, and the Deutsche Forschungsgemeinschaft for financial support (project JO 278/12-1).

References

[1] J. Heo, R.M. Crooks, *Anal. Chem.* 77 (2005) 6843.

- [2] J. Kim, N. Singh, L.A. Lyon, *Angew. Chem. Int. Ed.* 45 (2006) 1446.
- [3] W. Lee, D. Choi, Y. Lee, D.-N. Kim, J. Park, W.-G. Koh, *Sens. Actuators B* 129 (2008) 841.
- [4] A. Kikuchi, T. Okano, *J. Controlled Release* 101 (2005) 69.
- [5] N.A. Peppas, J.Z. Hilt, A. Khademhosseini, R. Langer, *Adv. Mater.* 18 (2006) 1345.
- [6] Y. Qiu, K. Park, *Adv. Drug Delivery Rev.* 53 (2001) 321.
- [7] H.G. Schild, *Prog. Polym. Sci.* 17 (1992) 163.
- [8] G. Graziano, *Int. J. Biol. Macromol.* 27 (2000) 89.
- [9] G. Liu, G. Zhang, *Langmuir* 21 (2005) 2086.
- [10] R. Freitag, F. Garret-Flaudy, *Langmuir* 18 (2002) 3434.
- [11] D. Kuckling, H.-J.P. Adler, K.-F. Arndt, J. Hoffmann, M. Plötner, T. Wolff, *Polym. Adv. Technol.* 10 (1999) 345.
- [12] L.K. Ista, S. Mendez, V.H. Pérez-Luna, G.P. López, *Langmuir* 17 (2001) 2552.
- [13] Y.V. Pan, R.A. Wesley, R. Luginbuhl, D.D. Denton, B.D. Ratner, *Biomacromolecules* 2 (2001) 32.
- [14] S. Palacin, C. Bureau, J. Charlier, G. Deniau, B. Mouanda, P. Viel, *ChemPhys-Chem* 5 (2004) 1468.
- [15] G. Deniau, J. Charlier, B. Alvado, S. Palacin, P. Aplincourt, C. Bauvais, *J. Electroanal. Chem.* 586 (2006) 62.
- [16] B. Ngounou, S. Neugebauer, A. Frodl, S. Reiter, W. Schuhmann, *Electrochim. Acta* 49 (2004) 3855.
- [17] J. Reuber, H. Reinhardt, D. Johannsmann, *Langmuir* 22 (2006) 3362.
- [18] N. Baute, C. Jérôme, L. Martinot, M. Mertens, V.M. Geskin, R. Lazzaroni, J.-L. Brédas, R. Jérôme, *Eur. J. Inorg. Chem.* (2001) 1097.
- [19] G. Yildiz, H. Çatalgil-Giz, F. Kadırgan, *J. Appl. Electrochem.* 30 (2000) 71.
- [20] C.S. Lee, J.P. Bell, *J. Mater. Sci.* 30 (1995) 3827.
- [21] S.L. Cram, G.M. Spinks, G.G. Wallace, H.R. Brown, *J. Appl. Polym. Sci.* 87 (2003) 765.
- [22] J. Bünsow, D. Johannsmann, *Macromol. Symp.* 248 (2007) 207.
- [23] W. Kunz, J. Henle, B.W. Ninham, *Curr. Opin. Colloid Interface Sci.* 9 (2004) 19.
- [24] Y. Zhang, S. Furryk, D.E. Bergbreiter, P.S. Cremer, *J. Am. Chem. Soc.* 127 (2005) 14505.
- [25] Q. Zou, B.J. Bennion, V. Daggett, K.P. Murphy, *J. Am. Chem. Soc.* 124 (2002) 1192.
- [26] J.D. Batchelor, A. Olteanu, A. Tripathy, G.J. Pielak, *J. Am. Chem. Soc.* 126 (2004) 1958.
- [27] M.C. Gurau, S.-M. Lim, E.T. Castellana, F. Albertorio, S. Kataoka, P.S. Cremer, *J. Am. Chem. Soc.* 126 (2004) 10522.
- [28] M. Boström, D.R. Williams, B.W. Ninham, *Phys. Rev. Lett.* 87 (2001) 168103.
- [29] A. Suzuki, Y. Kobiki, M. Yamazaki, *Jpn. J. Appl. Phys.* 42 (2003) 2810.
- [30] Ç. Sayil, O. Okay, *Polym. Bull.* 45 (2000) 175.
- [31] W.-F. Lee, S.-H. Yen, *J. Appl. Polym. Sci.* 78 (2000) 1604.
- [32] N. Ishida, S. Biggs, *Macromolecules* 40 (2007) 9045.
- [33] Y.K. Jhon, R.R. Bhat, C. Jeong, O.J. Rojas, I. Szleifer, J. Genzer, *Macromol. Rapid Commun.* 27 (2006) 697.
- [34] The value of 1 g/cm^3 for the density of the hydrogel is an assumption. The true density of the swollen film is not known (but close to one). Usually, the uncertainty in ρ_f is less important than the uncertainty in the viscoelastic contributions to d_s .
- [35] S. Camerlynck, P.A.G. Cormack, D.C. Sherrington, G. Saunders, *J. Macromol. Sci. Phys.* 44 (2005) 881.
- [36] The samples shown in Fig. 6 were prepared under basic conditions. The results cannot directly be compared to Fig. 4.